Title TBD

Author List TBD

November 10, 2014

1 Introduction

Observations of slow-slip and low-frequency earthquakes in nature suggest that fault failure encompasses a spectrum of slip modes [7, 6, **?**, 2]. While the explanations for non-traditional earthquakes remain a topic of debate [4], an ever increasing pool of data shows them to be found across the globe in a variety of tectonic settings (REFS). There is currently no way to know if the large amounts of elastically stored energy in a fault zone will always be released in slow-slip events or if fault behavior can transition to produce large earthquakes. It is difficult to study fault zone behavior and evolution given that large faults may have a recurrence interval of hundreds of years and that fault slip occurs deep enough in the Earth that we must rely on instrumentation located kilometers away. Laboratory stick-slip is often used to model and study repeating earthquake behavior (Brace and Byerlee, 1969; Johnson et al., 2013). Frictional stability of a system bifurcates at a critical stiffness , k_c [3]. For systems in which $k > k_c$, linearly stable response, while systems with $k < k_c$ are dynamically unstable [8]. Behavior at and near k_c is not well understood, but transitional behaviors such as sinusoidal stress variations and slow-slip have been observed [4, 1, 5] Our results show the critical stiffness to be the controlling factor for slip mode, itself influenced by environmental factors such as pore pressure and second order frictional properties of the gouge.

2 Body

Biaxial double-direct shearing experiments were performed with humidified Min-U-Sil® simulated fault gouge. Force and displacement are recorded on both axes, as well as a measurement of the shearing block position (Fig.1). System compliance can be modified by changing the normal stress or the material of which the shearing block is made (steel or cast acrylic).

Experiments performed under stiff system conditions exhibited linearly-stable behavior in response to order of magnitude velocity perturbations. Linearly-stable response is characterized by direct matching of the loading and system velocities and a transitory frictional response. Experiments of identical conditions, but in a more compliant system exhibited emergent unstable behavior, beginning with frictional oscillations, and transitioning to dynamic frictional failure. Oscillations and dynamic failure are characterized by relatively rapid accelerations and decelerations of the system above/below the load point velocity when the material yields under excessive shear force. Experiments with further increased compliance exhibited very rapid dynamic failure that was audible and classified as fast stick-slip.

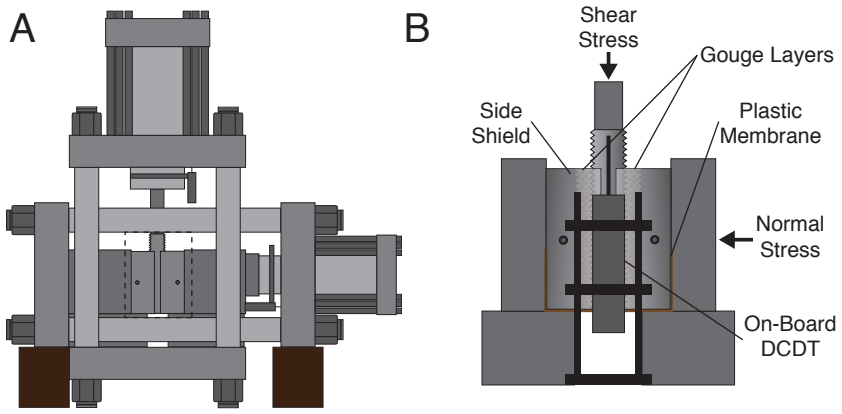

Figure 1: The biaxial deformation apparatus (A) and sample configuration (B). Two large hydraulic pistons are servo-controlled in either force or displacement control modes. Double direct shear samples are supported by steel blocks. Samples use metal side shields and a plastic membrane to reduce gouge extrusion. Local displacement transducers (DCDTs) can be referenced to the center block to negate apparatus stiffness corrections and measure deformation of the center block.

System stiffness measured in cycles of unloading and reloading the shear stress provide an estimate of aggregate stiffness for all experiments regardless of failure behavior. Stiffnesses recovered from the loading portion of individual stick-slip events show very low stiffnesses during early frictional oscillations and emerging slow-slip due to the non-static nature of the system. These values of "working stiffness" do not represent the overall stiffness of the system, but a stiffness influenced by continued slip and creep. As dynamic failure reaches a steady state, we see agreement between the two methods of stiffness measurement.

For experiments exhibiting stable sliding behavior, velocity steps were imposed to obtain the rate-and-state frictional parameters of the material and system. The a parameter provides a measure of the direct effect in response to a velocity step, and b provides the magnitude of friction evolution there-after. The difference of a and b, then yields a quantitative measure of how strongly velocity strengthening or velocity weakening a material is. The critical slip distance, Dc, is often considered to be the slip required to renew the contact population in a granular material. In our experiments, a remains relatively constant with displacement, but b evolves asymptotically upwards with increasing shear displacement. During this transitional period, the critical slip distance evolves downwards.

The transition from velocity strengthening to velocity weakening and corresponding decrease in k_c increase the value of the predicted critical stiffness. When the critical stiffness intersects the measured system stiffness, we begin to see frictional oscillations and dynamic failure. The larger the departure from $k = kc$, the more dramatic the behavior. Very stiff systems show no tendency to produced damped oscillations after a velocity step. Very compliant systems exhibit fast dynamic failure. (Fig. 2)

An examination of the requirements for unstable behavior yields two suggested conditions: 1) that the material be velocity neutral to velocity weakening, and 2) that the system stiffness be at or below the critical stiffness. Velocity weakening is a necessary, but insufficient condition for unstable behavior. If a material is velocity strengthening, any acceleration leading to slip is immediately arrested by increased shearing resistance. The stiffness of the system governs the rate at which

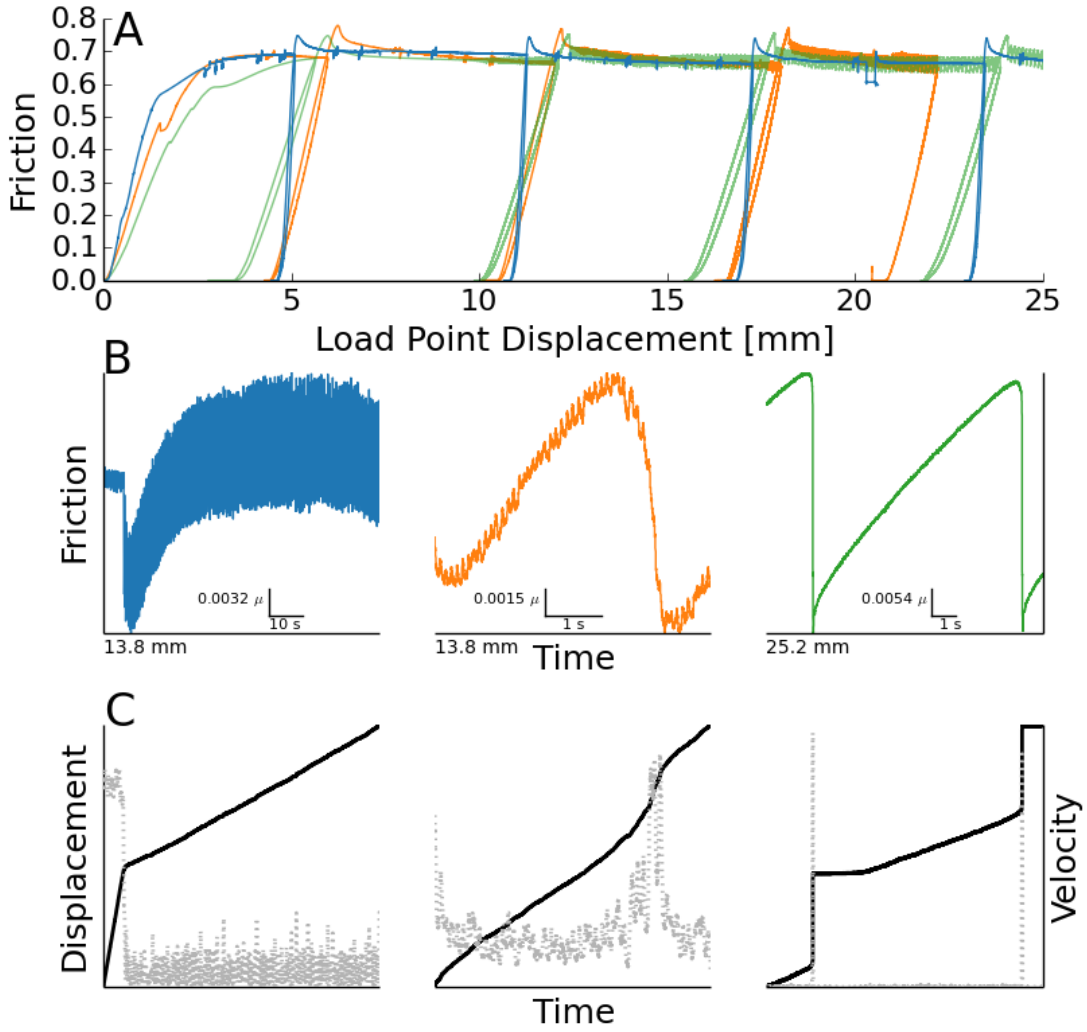

Figure 2: A) Run-plots of experiments p4309 (blue), p4311 (orange), and p4316 (green). Different working stiffnesses can be observed as the slope of unload/reload segments. B) All steel blocks produced stable responses to velocity steps. C) Destiffening the system with an acrylic center block produced non-audible slow-slip events. D) Further destiffening with an acrylic center block and increased normal stress produced audible fast stick-slip events.

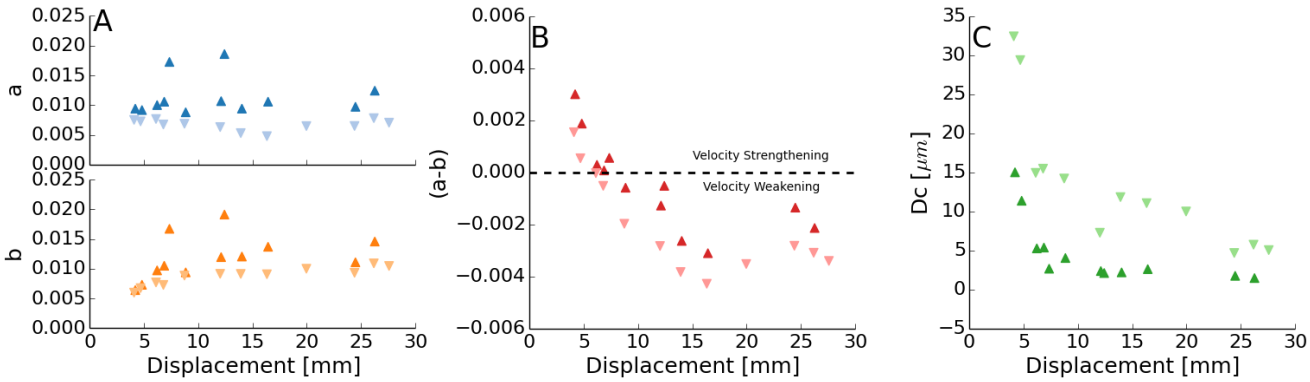

Figure 3: Rate-and-state friction parameters obtained from velocity step inversions. All inversions were accomplished with a fixed stiffness of 5.5e-3/um. A) rate-and-state parameter a remains relatively constant with displacement and shows a systematic behavior with higher values of a always being observed during velocity up-steps. The b parameter shows a similar behavior, but also increases with displacement, reaching a steady-state value around 10 mm displacement. B) The sample transitions from velocity strengthening to velocity weakening behavior at around 10 mm and remains velocity weakening for the remainder of the experiment. C) Critical slip distance estimates show considerable scatter, but do reduce to a steady-state value of 5-10 um.

energy stored as strain can be released. If the energy release occurs in such a way that the drop in shear resistance with displacement occurs faster than the drop in applied shearing force with displacement, the system can support unstable failure.

3 Discussion

Increases in measured aggregate system stiffness could be due to layer compaction due to grain rearrangement, layer thinning with increased shear strain, possible grain comminution and increased packing, localization of shear, and reduction of compliant material above sample due to geometric effects with shear. Of these, layer compaction, thinning, and shear localization are believed to be the largest.

Our observations of transitional behavior beginning when $k \sim k_c$ suggests that k_c is a valid proxy for the stability of a system, marking a transitory zone between stable sliding and stick-slip that encompasses slow-slip and oscillatory behavior. We also observe that the critical stiffness of a system evolves with shear strain, suggesting that tectonic faults may change behavior as they accumulate slip and become mature fault zones. Laboratory results can also be connected to observations in nature through the critical patch size. Critical patch size grows with increasing k_c and/or increasing normal stress. Extending this to large patch sizes hypothesized for slow-slip events suggests lowered normal stress, possibly due to high pore-pressures and/or low critical stiffness values.

4 Methods

All experiments were performed on a servo-controlled biaxial shearing apparatus. Displacements on the normal and shearing axes were measured by Direct Current Displacement Transducers (DCDTs) referenced at the end-platens and ram nose. The displacement of the shearing block was measured with a DCDT referenced at the end-platen and the top of the shearing block. Loads applied to the sample were measured with strain gauge load cells. All transducers are semi-annually calibrated with a traceable transfer standard.

Samples were prepared in the double-direct-shear geometry using steel or titanium side blocks and steel or acrylic shearing blocks. All blocks were grooved 0.8 mm deep at 1 mm spacing to reduce boundary effects. The sample area was 10 x 10 cm and filled with Min-U-Sil to a thickness of 3 mm. Granular layers were left in a sealed container overnight with a solution of anhydrous sodium carbonate to humidify the samples.

After samples were loaded into the load frame, a constant normal stress was applied and maintained by the servo system in a force feedback control mode. Samples were allowed to compact and accomodate grain rearrangement before shearing began. Shearing is conducted at a fixed rate of 10 $\mu m/s$ in displacement feedback control mode.

Stiffness of the system was altered by changing the applied normal stress and by changing the material of the shearing block. Increasing normal stress decreases the effective stiffness of the system, as does switching the steel forcing block for a cast acrylic block.

Layers were built of Min-U-Sil® 40 fine ground silica from the U.S. Silica® company Berkeley Springs, West Virginia plant. The median diameter of grain is 10.5 μm. The product is 99.5 % SiO_s, with traces of metal oxides making up the remainder.

System stiffnesses from unload/reload shear stress cycles were calculated by a least-squares linear fit in friction vs. displacement for the interval $\mu = 0.3 - 0.4$. Stiffnesses from the loading portion of slow-slip and stick-slip events were obtained with a derivative based algorithm described by Leeman et al. (In Review). Rate-and-state models were fit with both the Dieterich and Ruina laws, with comparable results. Inversions were done with an iterative singular value decomposition technique.

5 References

References

[1] Heslot F. Perrin B. Baumberger, T. Crossover from creep to inertial motion in friction dynamics. *Nature*, 367(6463):544–546, 1994.

[2] Gregory C. Beroza and Satoshi Ide. Slow earthquakes and nonvolcanic tremor. *Annual Review of Earth and Planetary Sciences*, 39(1):271–296, 5 2011.

[3] Ji-Cheng Gu, James R Rice, Andy L Ruina, and Simon T Tse. Slip motion and stability of a single degree of freedom elastic system with rate and state dependent friction. *Journal of the Mechanics and Physics of Solids*, 32(3):167–196, 1984.

[4] Bryan M. Kaproth and C. Marone. Slow earthquakes, preseismic velocity changes, and the origin of slow frictional stick-slip. *Science*, 341(6151):1229–32, 9 2013.

[5] Scuderi M.M. Marone C. Saffer D.M. Leeman, J.R. Stiffness evolution of granular layers and the origin of repetitive, slow, stick-slip frictional sliding. *Granular Matter*, Submitted.

[6] Kazushige Obara. Nonvolcanic deep tremor associated with subduction in southwest japan. *Science*, 296(5573):1679–81, 5 2002.

[7] Zhigang Peng and Joan Gomberg. An integrated perspective of the continuum between earthquakes and slow-slip phenomena. *Nature Geosci*, 3(9):599–607, 8 2010.

[8] Christopher H. Scholz. *The mechanics of earthquakes and faulting*. Cambridge university press, 2002.

6 Acknowledgements

The authors with to thank Steve Swavely for his support in the laboratory. This material is based upon work supported by the National Science Foundation under Grant No. DGE1255832. Any opinions, findings, and conclusions or recommendations expressed in this material are those of the author(s) and do not necessarily reflect the views of the National Science Foundation. The work was also supported by funds from the GDL Foundation and Shell Oil.

7 Author Contributions

All authors contributed to data interpretation, analysis schema, and writing. J. Leeman conducted experiments and data analysis.

8 Competing Financial Interests

The authors declare no competing financial interests. Supplementary information accompanies this paper on www.nature.com/naturegeoscience. All data is avaliable for download, as well as Python scripts/notebooks to replicate data analysis on GitHub (www.github.com/jrleeman). Reprints and permissions information is available online at http://npg.nature.com/reprintsandpermissions. Correspondence and requests for materials should be addressed to J. Leeman.